Characterization of the low-lying 0^+ and 2^+ states in ^{68}Ni via β decay of the low-spin ^{68}Co isomer

F. Flavigny,[1,*] D. Pauwels,[1] D. Radulov,[1] I. J. Darby,[1] H. De Witte,[1] J. Diriken,[1,2] D. V. Fedorov,[3] V. N. Fedosseev,[4] L. M. Fraile,[5] M. Huyse,[1] V. S. Ivanov,[3] U. Köster,[6] B. A. Marsh,[4] T. Otsuka,[7,8] L. Popescu,[2] R. Raabe,[1] M. D. Seliverstov,[1,3,9] N. Shimizu,[7] A. M. Sjödin,[4] Y. Tsunoda,[8] P. Van den Bergh,[1] P. Van Duppen,[1] J. Van de Walle,[10] M. Venhart,[1,11] W. B. Walters,[12] and K. Wimmer[8,13]

[1]*KU Leuven, Instituut voor Kern- en Stralingsfysica, Celestijnenlaan 200D, 3001 Leuven, Belgium*
[2]*Belgian Nuclear Research Centre SCKCEN, Boeretang 200, B-2400 Mol, Belgium*
[3]*Petersburg Nuclear Physics Institute, NRC Kurchatov Institute, 188300 Gatchina, Russia*
[4]*EN Department, CERN, CH-1211 Geneva 23, Switzerland*
[5]*Grupo de Física Nuclear, Universidad Complutense, CEI Moncloa, 28040 Madrid, Spain*
[6]*Institut Laue-Langevin, 71 avenue des Martyrs, 38042 Grenoble, France*
[7]*Center for Nuclear Study, University of Tokyo, Hongo, Bunkyo-ku, Tokyo 113-0033, Japan*
[8]*Department of Physics, University of Tokyo, Hongo, Bunkyo-ku, Tokyo 113-0033, Japan*
[9]*Department of Physics, University of York, York YO10 5DD, United Kingdom*
[10]*PH Department, CERN, CH-1211 Geneva 23, Switzerland*
[11]*Institute of Physics, Slovak Academy of Sciences, SK-84511 Bratislava, Slovakia*
[12]*Department of Chemistry and Biochemistry, University of Maryland, College Park, Maryland 20742, USA*
[13]*Physik Department E12, Technische Universitat Munchen, D-85748 Garching, Germany*

(Received 12 November 2014; revised manuscript received 21 January 2015; published 9 March 2015)

The low-energy structure of the neutron-rich nucleus ^{68}Ni has been investigated by measuring the β decay of the low-spin isomer in ^{68}Co selectively produced in the decay chain of ^{68}Mn. A revised level scheme has been built based on the clear identification of β-γ-$E0$ delayed coincidences. Transitions between the three lowest-lying 0^+ and 2^+ states are discussed on the basis of measured intensities or their upper limits for unobserved branches and state-of-the-art shell model calculations.

DOI: 10.1103/PhysRevC.91.034310 PACS number(s): 23.40.−s, 23.20.Lv, 21.10.−k, 27.50.+e

I. INTRODUCTION

The manifestation of shape coexistence in atomic nuclei is a unique phenomenon strongly related to shell gaps and the residual proton-neutron interaction, leading to particle-hole excitations and deformation [1]. Evidence for this can be found all over the nuclear chart in regions close to shell- or subshell closures. The region around ^{68}Ni is interesting in that respect due to the $Z = 28$ spherical magic number and the $N = 40$ oscillator shell closure. The latter separates the negative parity pf neutron orbitals from the positive parity $g_{9/2}$ orbital. A strong fingerprint for shape coexistence in even-even nuclei is the occurrence of low-lying 0^+ states like in the most notorious case of ^{186}Pb where, next to the 0^+ ground state, two 0^+ have been identified as the lowest excited states [2].

In ^{68}Ni, the first excited state is also a 0^+ state at quite low energy and was initially positioned at 1770(30) keV [3]. Its energy was corrected recently as 1603.5(3) keV in an in-beam γ spectroscopy study producing ^{68}Ni [4], as 1605(3) keV in a β-decay study [5], and also in the present study as 1603.6(6) keV. According to shell model calculations, the structure of this 0^+_2 state consists basically in 2p-2h excitations from the $Z = 28$ and $N = 40$ closed shells with more weight of neutron excitations [4,6–9]. This hypothesis has just been confirmed by a ^{66}Ni$(t,p)^{68}$Ni reaction study performed at REX-ISOLDE on the basis of the relative cross sections to the 0^+_1 and 0^+_2 states [10]. The third 0^+ level at 2511 keV is not directly situated above the second one but separated by the first 2^+ state at 2033 keV. The 0^+ spin-parity of the 2511-keV state was proposed following the β-decay study of ^{68}Co [11] and confirmed in a multinucleon transfer reaction through γ-ray angular correlations [12]. Configurations involving substantial proton excitations from the $Z = 28$ closed shell represent one of the possible origins for a 0^+ excited state. Looking at neighboring odd-mass nuclei, the position of a π(2p-2h) state is estimated using the prescription given in [13] by summing the excitation energies of the possible π(1p-2h) and π(2p-1h) in, respectively ^{67}Co [14] and ^{69}Cu [15,16] which led to 2202 keV [17]. Experimentally, Dijon *et al.* [18] proposed a candidate at this energy for such a highly deformed π(2p-2h) proton intruder state using a multinucleon transfer reaction but no supporting evidence was found for this state in a subsequent study [12]. Importantly, only shell model calculations including proton excitations predict a third 0^+ state between 2.5 and 3 MeV but its configuration involves both π(2p-2h) and ν(4p-4h) excitations [5–8].

When it comes to 2^+ states, two of them have been identified at rather low energy. The first one located at 2033 keV was identified by Broda *et al.* [19] much higher than in the neighboring nickel isotopes, while its $B(E2,0^+_1 \rightarrow 2^+_1)$ is

*Present address: Institut de Physique Nucléaire d'Orsay, CNRS-IN2P3, 91406 Orsay, France; flavigny@ipno.in2p3.fr

relatively low [20,21] and the second one proposed in Ref. [11] is located at 2743 keV. Several other levels of different spins and parity were identified by β-decay studies [5,11] and in-beam studies [4,19,22,23].

With three firmly established 0^+ and two 2^+ states below 2.8 MeV, it becomes imperative to identify their associated structures and to characterize their inter- and intradecay patterns. In this article, we will present the results of a β-decay study, performed at ISOLDE, CERN, focused on this low-spin level structure in ^{68}Ni by selectively producing only the low-spin isomer in ^{68}Co. Out of the improved level scheme and the selective population of low-spin states only, precise intensities were determined for the observed transitions de-exciting the different 0^+, 2^+, and 4^+ together with upper limits of the nonobserved but possible transitions. The extracted transition rates will be compared with theoretical predictions leading to conclusions on the possible underlying character of the different configurations.

II. EXPERIMENT

At ISOLDE, CERN, $T_{1/2} = 28(3)$ ms [24] ^{68}Mn nuclei were produced in a 1.4 GeV proton-induced ^{238}U fission reaction and selectively ionized with the resonance ionization laser ion source (RILIS) [25]. After mass separation, the ^{68}Mn ion beam was implanted on an aluminized mylar tape, inside a movable tape station surrounded by three plastic $\Delta E\,\beta$ detectors and two MiniBall γ-detector clusters [26] in close geometry. More information on the detection setup can be found in [27]. The experimental data were recorded on an event-by-event basis using digital electronics, with no hardware trigger applied. The acquisition of the decay data was based on the CERN proton supercycle structure. A supercycle (SC) can contain up to 40 proton pulses (PP) distributed with a difference of 1.2 s between each of them. In the present experiment, the proton pulses (2.8×10^{13} p/pulse) sent to the target were every odd pulse starting at the third PP and ending with the 33th PP. After each SC, the tape was moved in order to remove long-living activity. The implantation was stopped 69 ms after every PP impact. This limited implantation time of about $2.5 \times T_{1/2}(^{68}\text{Mn})$ was applied in order to suppress the implantation of isobaric $T_{1/2} = 67.71(8)$ min ^{68}Ga [28], produced in the spallation of ^{238}U and surface ionized [29] in the hot cavity of RILIS. This background was measured by periodically blocking one of the RILIS laser beams (*laser-off* mode).

Decay data corresponding to a total measuring time of 18 152 s in the *laser-on* mode and 5036 s in *laser-off* mode were recorded. An average beam intensity of 3.1(3) implanted ^{68}Mn ions per second has been obtained during this measuring time when the laser ionization was optimal. The acquisition time after each PP extended to 2.2 s. This means that the first part of this acquisition time (0 to 350 ms) is dominated by the decay radiation of $T_{1/2} = 28(3)$ ms ^{68}Mn and its 188(4) ms [28] ^{68}Fe daughter. Therefore for a number of cases, only the latter part (350–2200 ms) was used to study the decay of the $T_{1/2} = 1.6$ s [11] low-spin isomer of ^{68}Co in clean conditions. Since cobalt isotopes are only very slowly released and not ionized by the ISOLDE target-ion-source system used in the present experiment, the only production of ^{68}Co comes through the decay of even-even ^{68}Fe. In this decay the $T_{1/2} = 0.23(3)$ s [11] ^{68}Co (7^-) β-decaying state is not populated. Conflicting results do exist on the spin determination of the low-spin β-decaying state in ^{68}Co: (3^+) according to Mueller *et al.* [11] and (1^+) according to Liddick *et al.* [30]. The results obtained here on this controversy will be presented below and are based on the purity of the ^{68}Mn sources and the possibility of observing the decay of the respective daughters. This allows us to draw conclusions on the completeness of the decay schemes, addressing missed γ-ray intensity and direct ground-state feeding. Extensive new decay information of ^{68}Mn and ^{68}Fe has also been acquired but will be published elsewhere.

III. RESULTS

By using coincident events in which two plastic detectors were hit within 2 μs and by inspecting the time difference between these two hits, 590 coincident events were observed outside of the prompt window [−125,50] ns (the counts in the prompt window are due to scattering of β particles from one detector to the other). Random coincidences in this off-prompt time window contribute to 6(2)% of these events and were determined using data collected with a ^{67}Mn beam during the experiment. The delayed time difference between the two coincident plastic signals for these 590 events is presented in Fig. 1 and the deduced half-life [235(23) ns] is in reasonable agreement with the known half-life of the first excited 0^+ state of 270(5) ns [20]. These events are understood as the delayed coincidence between ^{68}Co β rays and delayed $E0$ conversion electrons or e^-/e^+ signals from the electron-positron pair creation in the decay of the first excited 0^+ to the ground state in ^{68}Ni.

It is possible to observe the γ transitions coincident to this selective signal in the MiniBall detectors. This coincident spectrum is shown on Fig. 2 where three peaks can be identified: (i) the 511-keV line originates from the positron annihilation radiation after the pair creation decay of the 0_2^+;

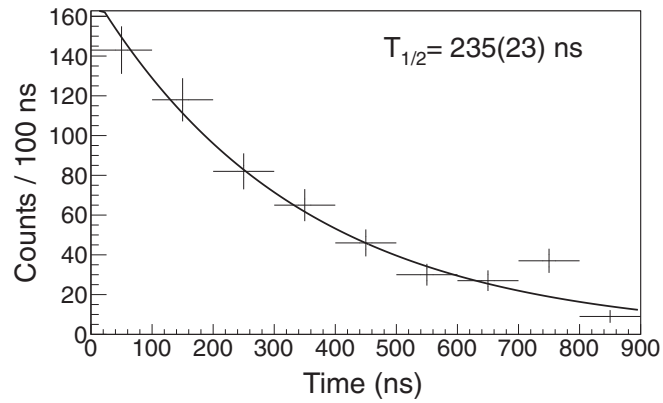

FIG. 1. Time spectrum between two consecutive signals in the plastic detectors in the time region [−1000, −125] ns and [+50, +1000] ns, outside the prompt time distribution to exclude β scattering from one detector to another.

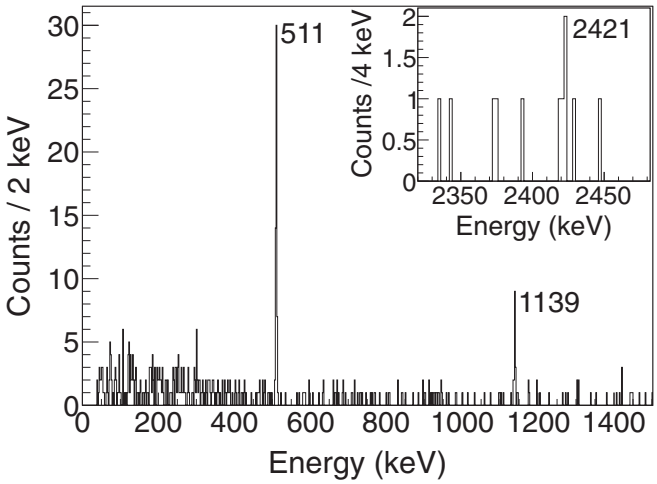

FIG. 2. Gamma spectrum in coincidence with the decay radiation from the 0_2^+ to 0_1^+ in ^{68}Ni. The time condition required is that the γ ray is detected within 600 ns after one of the two plastic signals (^{68}Co β rays or delayed $E0$ signal, see text).

(ii) the 1139-keV line was observed in the previous decay study [11] but its placement was unsure; (iii) a weak 2421-keV line. Both the 1139 and the 2421 keV γ lines fit in the level scheme presented in Fig. 4 fixing the energy of the first excited 0^+ state at 1603.6(6) keV, well below the earlier value of 1770(30) keV [3]. This repositioning of the second 0^+ agrees well with recently published values from an in-beam γ-spectroscopy study and β decay, respectively [4,5]. With the newly positioned 2421-keV transition and the identification of a weak 4027-keV branch to the ground state, three transitions from the 4025.6(4) keV state to 0^+ states are now established. Based on this pattern, a tentative spin assignment of (2^+) is preferred to the former $(2^+,3^+,4^+)$ hypothesis from Ref. [11].

Transitions associated with the decay of ^{68}Co were also identified by comparing β-gated γ spectra with and without lasers tuned to resonantly ionize manganese as shown on Fig. 3. Due to the selective production of the low-spin β-decaying state of ^{68}Co, several problems related to the previous study [11] were solved. This study was hampered by doublets such as the 710-keV line, occurring both in the low-spin and high-spin decay (see remark c in Table III of [11]), and tentatively placed transitions. The 1139-keV and the 694-keV line tentatively placed on the 2847-keV $T_{1/2} = 0.86(5)$ ms [19] 5^- level were apparently not observed in deep-inelastic scattering studies although tentatively assigned (3^-) and (4^-) levels were identified feeding the 5^- level [12,23]. The 1139-keV transition is now firmly placed on the 0_2^+ level while the 694-keV line is now identified as a γ line following β-delayed n emission and de-exciting the 694-keV $5/2^-$ level in ^{67}Ni. Furthermore by applying a slow β-γ coincidence (1–2580 μs) the presence of the 814-keV transition could be proven and thus the intensity passing through the 2847-keV isomeric 5^- level deduced. Similarly using the 590 slow plastic-plastic coincidence events, the amount of intensity passing through the 1604-keV isomeric 0_2^+ level was obtained. By inspecting

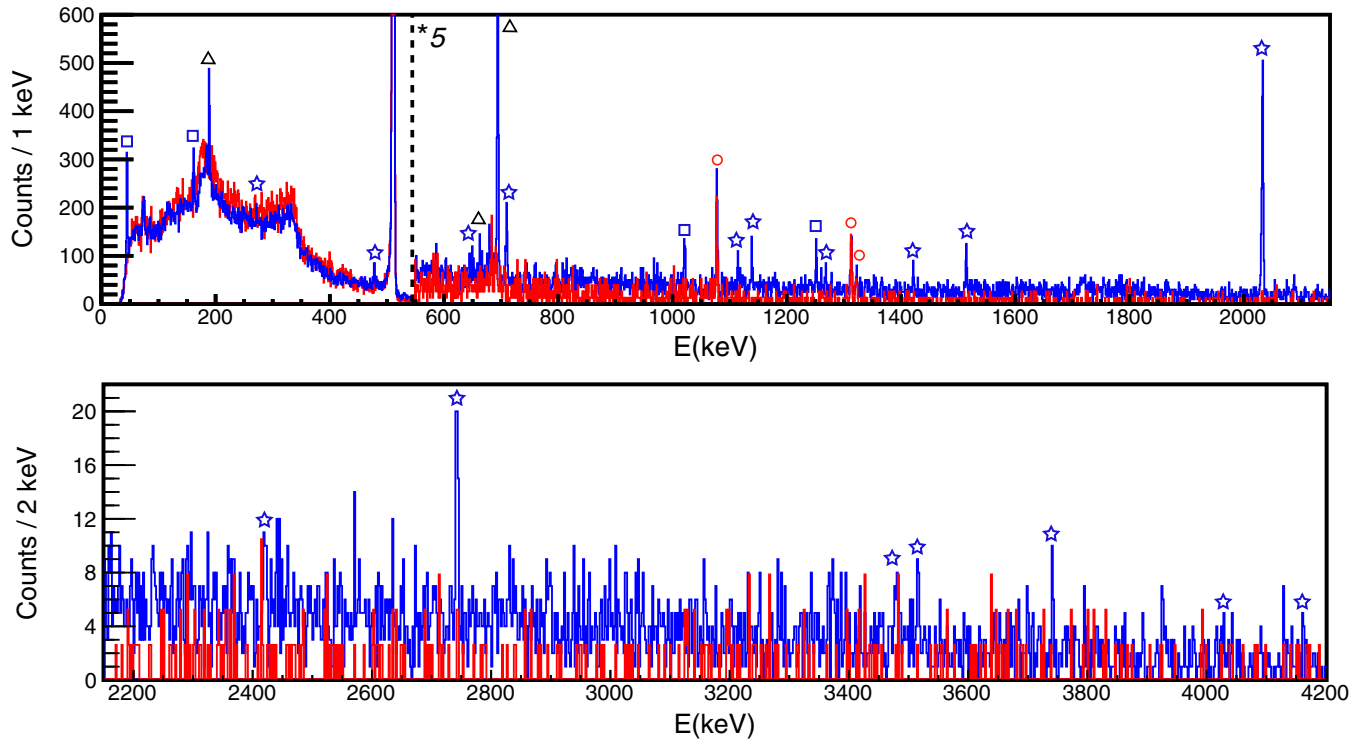

FIG. 3. (Color online) β-gated γ-ray spectrum in the time window [350, 2200] ms after the proton pulse impinged on the target when (blue) lasers are tuned to resonantly ionize Mn and (red) lasers are off. The laser-off spectrum was scaled to the laser-on one using the 1313-keV peak from ^{136}I for comparison. Symbols indicate lines associated with: ^{68}Co decay (stars), ^{68}Fe decay (squares), ^{67}Fe and ^{67}Co decay after β-delayed neutron emission (triangles), laser off ^{68}Ga and ^{136}I contaminants decay (circles).

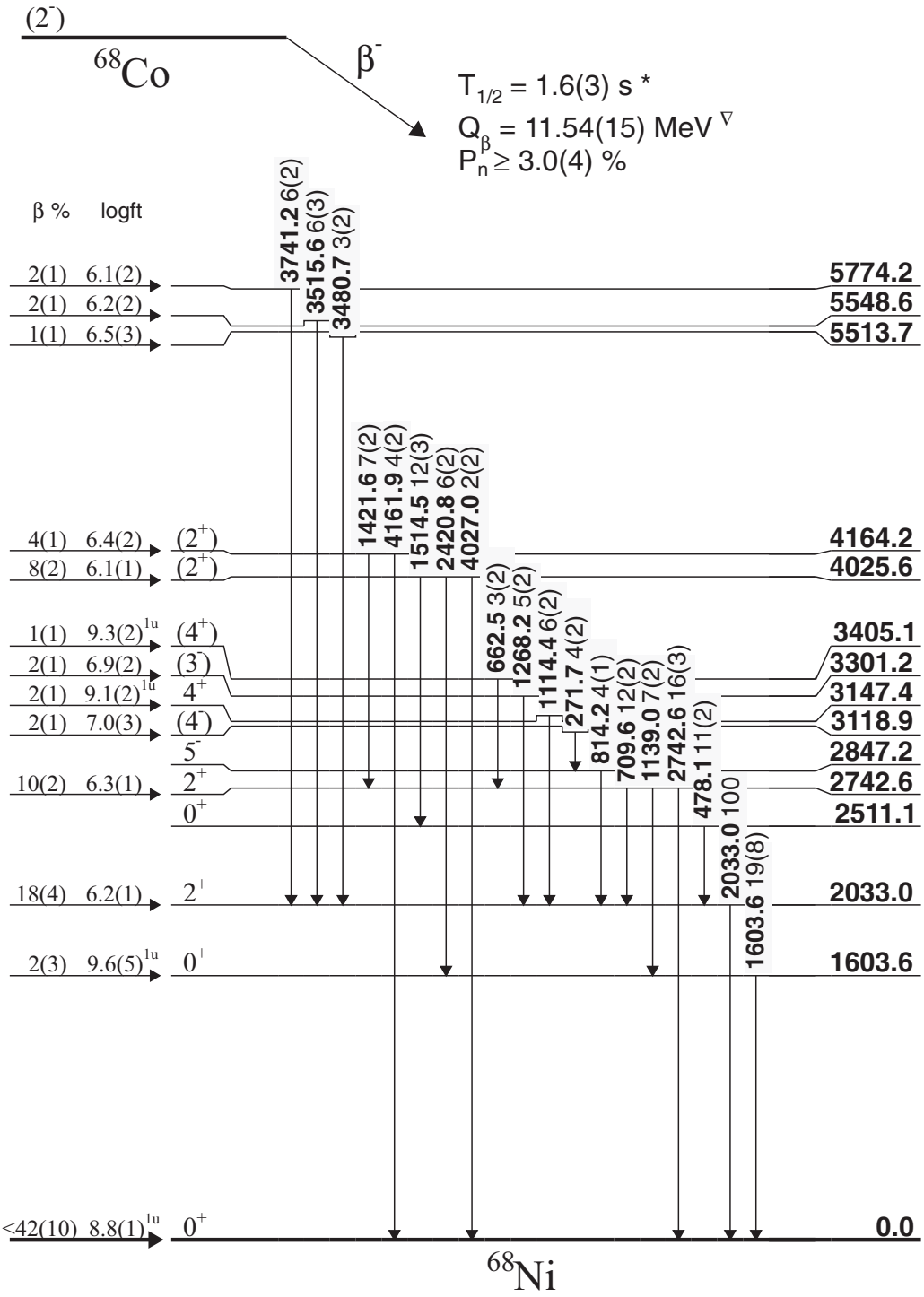

FIG. 4. Decay scheme of ^{68}Co. All the β-feeding percentages should be considered as upper limits (see text) and the missed feeding (possibly β, $E0$, or γ feeding) was determined using the method of Ref. [27]. Tentative spin-parity assignments in brackets for higher spin states (4^-,3^-,4^+) comes from Refs. [12,23]. When indicated with a *1u* exponent, log ft values were taken assuming a first-forbidden unique transition. Asterisk (*) from Ref. [11], upsidedown triangle ($^\nabla$) from Ref. [32].

the full $A = 68$ (Mn-Fe-Co-Ni) decay chain, including also the $A = 67$ (Fe-Co-Ni) decay chain populated through β-delayed n-emission of ^{68}Mn and ^{68}Co, it was possible to calculate the unobserved intensity [42(10)%] in the decay of the ^{68}Co low-spin isomer, further called *missed feeding* which can be due to (i) direct β feeding of the ^{68}Ni ground state, (ii) direct β-delayed-neutron feeding to the ground state or isomeric state at 1008 keV in ^{67}Ni, (iii) missed $E0$ decay (note that in [11] a strong 511-keV component could not be explained), or (iv) missed γ rays feeding the ground or isomeric states

in ^{67,68}Ni. The method we used is described in [27]. Unfortunately, due to the strong presence of the β^+-decaying ^{68}Ga isobaric contaminant, it was impossible to verify the important 511-keV γ-ray intensity observed in the decay of the low-spin ^{68}Co state by Mueller *et al.* [11], explained as coming from electron-positron annihilation after internal pair creation caused by an $E0$ transition. In that work it was concluded that the prompt coincidence with β particles excluded the isomeric 0_2^+ level as the origin. However, since in that work identical β detectors were used in the same configuration as in the present work, it is now clear that the rejection of the 0_2^+ level as origin for the 511 keV γ-ray intensity is not fully justified. As can be seen in Fig. 2, a clear peak at 511 keV is present and is explained by the fact that the efficiency for detecting one or both particles from the internal pair creation in the plastic detectors is not negligible. The 2511-keV 0_3^+ level could also be a possible candidate as origin of some of this 511-keV events and was discussed in [11] however without firm conclusions. Here we can add that the 2σ upper limit of 2% on the relative intensity of the $0_3^+ \rightarrow 0_2^+$ branch suggests that this transition does not contribute significantly to the intensity of the 511-keV peak.

In Table I, energies and intensities are summarized for all γ lines observed in this decay study together with upper limits within 95% confidence level (2σ) for a number of possible but not observed transitions. A comparison with the intensities from the previous β-decay study of Mueller *et al.* [11] is shown in the last column. The fact that the relative intensity of the 694-keV line is larger in our work is due to the important β-delayed neutron branch of ^{68}Mn also leading to ^{67}Co and β-decaying to ^{67}Ni. The 7.6(3)% intensity of Ref. [11] has therefore been used to calculate the feeding percentages in the level scheme presented on Fig. 4 and to estimate a lower limit on the β-delayed neutron branch $P_n \geqslant 2.9(4)\%$. The 710-keV intensity also differs significantly but, as mentioned before, the intensity of Ref. [11] has been obscured due to the presence of a doublet. Note that in the work of Recchia *et al.* [4], the direct measurement of the 710-keV line was also hampered by contaminants.

The β-feeding intensities given for most of the levels must be considered as upper limits and consequently the deduced $\log ft$ values are lower limits. Mueller *et al.* [11] concluded that the apparent β-feeding of the 2033-keV, 2511-keV, and 2743-keV levels was rather due to unobserved γ rays and stated that "about 50% of the β decay of the low-spin state likely proceeds via unresolved levels". We mentioned previously that tentative contradictory spin-parity assignments (3^+) and (1^+), respectively, in Refs. [11] and [30], were made for the ^{68}Co low-spin state only on the basis of the β-feeding pattern. Three arguments would in principle support the presence of a strong Pandemonium effect [31]: (i) the very high Q value of 11.54(15) MeV [32], (ii) the fact that levels with spins up to 5^- are observed in the decay of the low-spin isomer, (iii) the 42(10)% of missed feeding. New experimental data has emerged that shed doubt on the (3^+) assignment originating from a $\pi(f_{7/2})^{-1}\nu(p_{1/2})^{+1}$ or $\pi(f_{7/2})^{-1}\nu(f_{5/2})^{+1}$ coupling, for the low-spin β-decaying states in ^{66}Co and ^{68}Co [11]. This original (3^+) assignment by Mueller *et al.* for the ^{66}Co ground state was based on the strong feeding of an assumed

TABLE I. (top) Summary of γ energies and intensities in ^{68}Ni relative to the $(2_1^+ \rightarrow 0_1^+)$ γ-ray transition obtained in this work compared to the published results of Mueller*et al.* for the decay of the low-spin isomer of ^{68}Co [11]. (bottom) Intensities and 2σ upper limits (95% CL) determined for different 0^+ to 0^+ decays.

E (keV)	J_i^+	J_f^+	$I_{\rm rel}$(%) (this work)	$I_{\rm rel}$(%) [11]
271.7 ± 0.5	(4^-)	5^-	4(2)	–
429.4 ± 0.8	2^+	0^+	< 0.7	–
478.1 ± 0.2	0^+	2^+	11(2)	15.5(7)
662.5 ± 0.7	(4^+)	2^+	3(2)	3.4(2)
694.1 ± 0.2			64(5)[a]	7.6(3)
709.6 ± 0.3	2^+	2^+	12(2)	6.0(4)
814.2 ± 0.6	5^-	2^+	4(1)	–
1114.4 ± 0.3	4^+	2^+	6(2)	9.7(5)
1139.0 ± 0.5	2^+	0^+	7(2)	6.2(4)
1268.2 ± 0.4	(3^-)	2^+	5(2)	–
1421.6 ± 0.4	(2^+)	2^+	7(2)	10.6(6)
1514.5 ± 0.3	(2^+)	0^+	12(3)	10.2(5)
2033.0 ± 0.1	2^+	0^+	100	100
2420.8 ± 0.6	2^+	0^+	6(2)	–
2742.6 ± 0.6	2^+	0^+	16(3)	14.7(8)
3480.7 ± 2.2		2^+	3(2)	7.4(7)
3515.6 ± 2.7		2^+	6(3)	5.5(7)
3741.2 ± 0.9		2^+	6(2)	10.3(7)
4027.0 ± 2.0	(2^+)	0^+	2(2)	–
4161.9 ± 2.4	(2^+)	0^+	4(2)	–

$E0$ decays

E(keV)	J_i^+	J_f^+	$I_{\rm rel}$ (%) (this work)
1603.6 ± 0.8	0_2^+	0_1^+	19(8)
908.0 ± 0.8	0_3^+	0_2^+	<2
908.0 ± 0.8	0_3^+	0_2^+	sum < 4
2511 ± 0.8	0_3^+	0_1^+	

[a]Line in ^{67}Ni from β-n branches in the whole $A = 68$ decay chain.

(3^+) spin-parity of the 2672 keV state in ^{66}Ni. The firm identification of a 0^+ spin-parity for this state [23] refutes the (3^+) assignment for ^{66}Co.

The recent discovery of a deformed $(1/2^-)$ isomer in ^{67}Co at an excitation energy of 492 keV above the $7/2^-$ ground state [14] opens up other proton-neutron coupling schemes. Liddick *et al.* [30] suggested a (1^+) assignment for the ground state of ^{66}Co and the low-spin isomeric state of ^{68}Co, originating from the coupling of a $[301]1/2^-$ neutron state with this $[321]1/2^-$ deformed proton level of ^{67}Co. However, there is a substantial difference between the β-decay feeding pattern of the ^{68}Co low-spin isomer as compared to the ones from the ^{64}Co 1^+ and ^{66}Co (1^+) ground states. In the beta decay of ^{64,66}Co, only 0^+ and 2^+ states in the daughter nickel isotopes were populated and the ground-state feeding correspond respectively to $\log ft$ values of 4.27(5) and 4.7(1) [33–35]. This points to a $\pi(f_{7/2})^{-1}\nu(f_{5/2})^{+1}$ based 1^+ ground state and allowed $\nu f_{5/2}$-$\pi f_{7/2}$ GT decay. On the contrary, the ^{68}Co low-spin decay scheme leads to direct and indirect feeding of higher spin states including 4^+ and 5^- states. Further, in spite of the larger Q_{EC} value (about 11.5 MeV for ^{68}Co versus 9.6 MeV for ^{66}Co) the half-life of the low-spin

TABLE II. Absolute $B(E2)$ in $e^2\mathrm{fm}^4$ and $B(E2)$ ratios $R(E_\gamma)$ for low-lying transitions in ^{68}Ni. Theoretical values for MCSM calculations using the revised A3DA interaction (see Ref. [6] for details) and SM calculations using the LNPS interaction from Ref. [8] are compared to experimental values. Effective charges $e_n = 0.5e$ and $e_p = 1.5e$ were used in the A3DA calculations.

J_i^+	J_f^+	E_γ(keV)	$E(J_i^+)$ (keV)			$B(E2, J_i^+ \to J_f^+)$			$R(E_\gamma)$		
			A3DA	LNPS	exp.	A3DA	LNPS	exp.	A3DA	LNPS	exp.
2_1^+	0_1^+	2033	2326	1989	2033.0(1)	15.1	41.0	51(12)[a]	1	1	1
	0_2^+	429	–	–	–	182	168	–	12.1	4.1	<17
0_3^+	2_1^+	478	2888	2629	2511.1(2)	0.21	15.1	–	–	–	–
2_2^+	0_1^+	2743	3145	2863	2742.6(3)	0.35	0.31	–	1	1	1
	0_2^+	1139	–	–	–	4.84	10.8	–	14	35	36(12)
	2_1^+	710	–	–	–	10.1	86.1	–	29	278	448^{+185}_{-311}
	0_3^+	232	–	–	–	774	757	–	2238	2442	$<9.10^4$
(2_3^+)	0_1^+	4027	3980	–	4025.6(4)	0.01	–	–	1	–	1.0(8)
	0_2^+	2421	–	–	–	0.01	–	–	1.2	–	36(18)
	2_1^+	1993	–	–	–	9.64	–	–	964	–	<78
	0_3^+	1515	–	–	–	2.45	–	–	245	–	831
	2_2^+	1281	–	–	–	3.26	–	–	326	–	<457
(2_4^+)	0_1^+	4162	4483	–	4164.2(5)	0.27	–	–	1	–	1
	0_2^+	2561	–	–	–	0.22	–	–	0.8	–	<9
	2_1^+	2131	–	–	–	2.19	–	–	8.1	–	<35
	0_3^+	1653	–	–	–	0.20	–	–	0.7	–	<104
	2_2^+	1422	–	–	–	4.79	–	–	17.6	–	346(172)
	(2_3^+)	139	–	–	–	6.22	–	–	22.9	–	–

[a]From Ref. [20].

isomer in ^{68}Co is an order of magnitude longer compared to ^{66}Co and, when assuming that the 42% missed feeding goes directly to the ground state, results in a $\log ft$ value of 6.3(1) much larger compared to the ground-state transitions in ^{64,66}Co decay.

With $N = 41$, another coupling scheme can evolve for the low-spin isomer of ^{68}Co. The low-lying deformed $[321]1/2^-$ proton configuration can couple to the downsloping $[431]3/2^+$ and $[440]1/2^+$ orbitals originating from the spherical $g_{9/2}$ state instead of the $[301]1/2^-$ as suggested in Ref. [30]. This would give 1^- or 2^- as possible spin-parity for the low-spin isomer in ^{68}Co but in view of the high-spin states populated in the β decay, a (2^-) assignment for the ^{68}Co low-spin state is preferred. Interestingly, the ^{68}Co low-spin β-decay scheme is similar to the β-decay scheme of the 2^- ground state of ^{78}As [36]. The 42% missed feeding is then assigned to <42% ground-state feeding as the pandemonium effect cannot be further quantified. As will be addressed in a forthcoming paper, the tentative (2^-) assignment is compatible with the new data obtained for the decay of ^{68}Fe into ^{68}Co.

IV. DISCUSSION

The reduced $E2$ transition probabilities $[B(E2)]$ from Monte Carlo shell model (MCSM) calculations described in Refs. [6,7] using the A3DA effective interaction with minor revisions and from shell model (SM) calculations using the LNPS effective interaction from Ref. [8] are summarized in Table II. A comparison to our results is made through $B(E2)$ ratios $[R(E_\gamma)]$ defined as $R(E_\gamma) = B(E2, E_\gamma, 2_i^+ \to I^+)/B(E2, 2_i^+ \to 0_1^+)$. For the 710-keV transition, we determined the $E2$ component of the transition using the $(E2/M1)$ mixing ratio $\delta = -1.5^{+0.9}_{-1.2}$ reported in Ref. [12]. The experimental $R(E_\gamma)$ ratios are also displayed in the level scheme of Fig. 5. It is worth mentioning here that both sets of calculations are phenomenological to certain extents but have not been designed to precisely reproduce suppressed (i.e., weak) transitions. Although we present below first comparisons for some of these weak transitions, they should not be considered alone as precise tests of the proposed Hamiltonians. In fact, there are strong cancellations

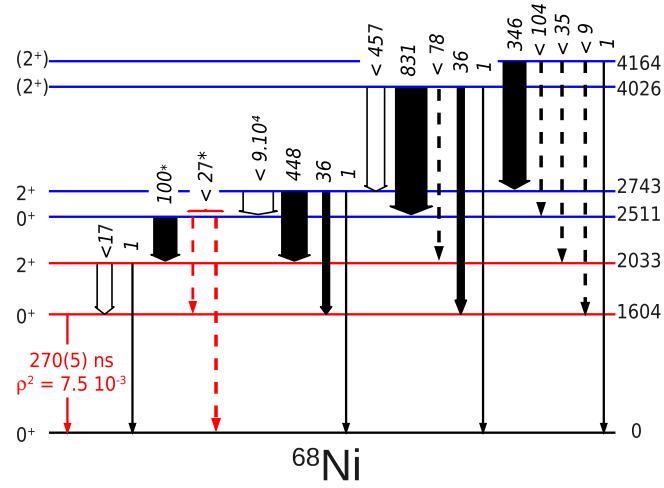

FIG. 5. (Color online) Level scheme of ^{68}Ni focused on the low-lying 0^+ and 2^+ states with their experimental $B(E2)$ ratios $[R(E_\gamma)]$ normalized to ground state transitions for each level. For the 0_3^+ state at 2511 keV, limits on branching ratios are quoted instead of $B(E2)$ ratios (indicated with an asterisk).

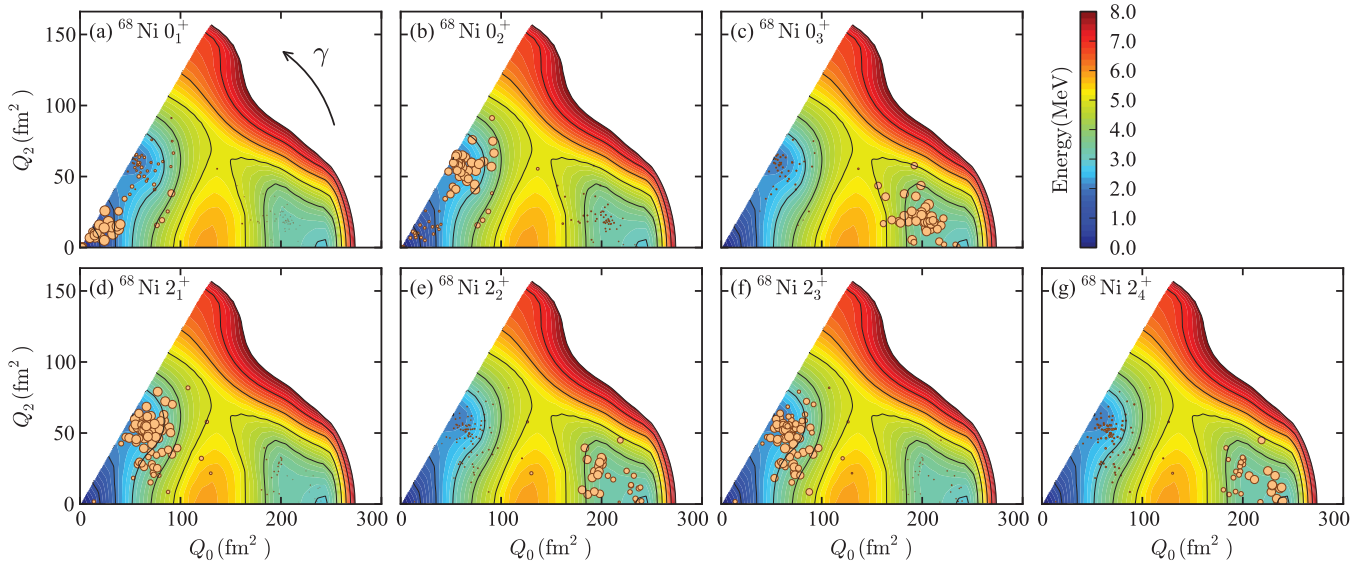

FIG. 6. (Color online) Potential energy surfaces (PESs) obtained from MCSM calculations [6] for the 0^+ and 2^+ states of ^{68}Ni, coordinated by the usual quadrupole moments Q_0 and Q_2 (or γ). Circles on the PES represent shapes of MCSM basis vectors (see Ref. [6] for more details).

among large matrix elements for such transitions and effective charges independent of orbits could become problematic. This problem is expected to be minor for strong transitions for which many effects are added and a kind of average matters for effective charges. In Table II, it can be illustrated for two enhanced $E2$ transitions ($2_1^+ \rightarrow 0_2^+$) and ($2_2^+ \rightarrow 0_3^+$) on which the two theoretical calculations agree with differences $\leqslant 10\%$.

Starting with the first 2^+ state, both theoretical calculations suggest a stronger connection with the 0_2^+ than with the ground state. An oblate deformation can be seen on the potential energy surface plot of Fig. 6 for the present MCSM calculation. From the nonobservation of the 429-keV transition ($2_1^+ \rightarrow 0_2^+$), the 2σ upper limit of 0.7(2)% relative to the 2033-keV branch leads to an upper limit of 17 on the $B(E2)$ ratio $R(429)$. This limit is here considerably improved compared to the 2σ limit of 41 from [4] but is still consistent with the theoretical calculations and shows that our sensitivity is below what would be needed to firmly examine these predictions. Concerning the only absolute value measured, $B(E2, 2_1^+ \rightarrow 0_1^+) = 51(12)\, e^2\,\text{fm}^4$, a reasonable agreement with calculations is found. More precisely, the LNPS prediction is compatible within a 1σ error but the A3DA value underestimates this $E2$ strength.

The 0_3^+ state at 2511 keV decays predominantly to the 2_1^+ state via the 478-keV transition with an intensity of 11(2)% relative to the 2033-keV transition and the sum of the other competing $E0$ branches to the 0_2^+ and 0_1^+ states have been constrained below 4%. Even if both shell model calculations agree on a strong prolate deformation for this 0_3^+ state (see for example Fig. 6), they predict significantly different $B(E2, 0_3^+ \rightarrow 2_1^+)$ values leading to partial half-lives of 108 and 1.5 ns, for A3DA and LNPS, respectively. The timing conditions obtained in the present experiment did not allow to further test these predictions but in Ref. [11] the 478-keV transition was observed as prompt with β particles to within the $\simeq$15 ns time resolution which is incompatible with the A3DA half-life.

For the 2_2^+ state, it is clear from both calculations that its $2_2^+ \rightarrow 0_2^+$ branch is predicted to be smaller than the $2_1^+ \rightarrow 0_2^+$ branch. On Fig. 6, this is illustrated by the difference between the predicted 2_2^+ prolate configuration and the 0_2^+ oblate configuration. In fact, the calculated absolute $B(E2)$ values for the 1139-keV transition to the 0_2^+ state are very small for both A3DA and LNPS interactions compared to the $2_2^+ \rightarrow 0_3^+$ transition (0.6% and 1.4%, respectively) and there is a factor of two difference between the two calculations. For this transition the LNPS calculation yields a $R(E_\gamma)$ value compatible with the experiment. For the $2_2^+ \rightarrow 2_1^+$ branch, we determined precisely the intensity of the 710-keV transition which deviates significantly from the value of Refs. [4,11] both blurred by contaminants. This leads to a higher $E2$ strength, significantly stronger than the $E2$ strength of the decays to lower 0^+ states even if a precise quantitative conclusion cannot be drawn due to the large uncertainty on the $E2/M1$ mixing ratio. The A3DA interaction produces a too small $B(E2)$ ratio of 29 for this 710-keV transition. Contrary to these suppressed transitions, it is crucial to stress that the $2_2^+ \rightarrow 0_3^+$ transition is a truly collective one in the theoretical calculations, as illustrated in the shape coexistence picture of Refs. [6,7]. While this transition is of paramount interest to explore unknown rich collectivities of nuclei around ^{68}Ni, a lack of sensitivity on its relative $B(E2)$ ratio (2σ upper limit of 9×10^4) comes mainly from the energy factor $(2743/232)^5$ and avoids an experimental test of this high degree of collectivity. Thus, the present work strongly stresses the necessity to perform a dedicated lifetime measurement of the 232-keV transition predicted around 1 ns for both calculations or a measurement of the absolute $B(E2)$ of any depopulating transition from this 2_2^+ state via Coulomb excitation to have an absolute reference.

Finally, concerning the two states at 4025.6(4) and 4164.2(7) keV proposed to be the (2_3^+) and (2_4^+) states, we

provide new information on their connections with lower-lying states. Especially for the (2_3^+) state, we measured for the first time the three connections to the 0^+ states. For the 4164-keV state, only the ground-state transition and a strong branch to the 2_2^+ state were observed. At this moment, only the MCSM calculations using the A3DA interaction are available for comparison with experiment and predict two extra 2^+ states at 3980 and 4483 keV. Interestingly, a qualitative agreement between experiment and theory is found concerning the decay of the (2_4^+) with an enhanced $E2$ strength towards the 2_2^+ state. In the calculation, the 2_2^+ and 2_4^+ states have a similar configuration corresponding to a strongly prolate shape [Fig. 6(g)]. Nevertheless, the situation for the (2_3^+) state predicted to have an oblate configuration [Fig. 6(f)] similar to the 2_1^+ state is more contrasted. The predicted $E2$ strengths to lower-lying 2^+ and 0^+ states are incompatible with measured $B(E2)$ ratios and upper limits from the nonobservation of corresponding transitions. This discrepancy is particularly clear for the $2_3^+ \rightarrow 2_1^+$ branch expected to be very strong due to similar oblate configurations [$R(E_\gamma)$ A3DA prediction of 964] but excluded by an upper limit of 78.

V. CONCLUSIONS

In summary, a revised level scheme has been built for ^{68}Ni based on the β-decay study of the low-spin isomer of ^{68}Co. The selective production of this isomer together with the identification of β-γ-$E0$ delayed coincidences allowed us to shed some light on the inconsistency of the spin determination between two previous β-decay studies [11,30] even if the identification of a strong missed feeding component avoid a firm spin-parity assignment. The clarification of connections between the different 2^+ and 0^+ states and the energy of the 0_2^+ isomer at 1603.6(6) keV agree well with recent published results [4,5]. The measured and calculated $B(E2)$ ratios using state-of-the-art shell model calculations do suggest similar structure between the 2_1^+ and 0_2^+ and between the 2_2^+ and 0_3^+. Candidates for the third and fourth 2^+ states and their characteristic decay paths have been identified. A first comparison to large-scale Monte Carlo shell model calculations shows a consistent picture for the 2_4^+ state, but substantial discrepancies for the decay pattern of the 2_3^+ state. Nevertheless, key experimental information is missing to firmly conclude on the coexistence of different shapes in ^{68}Ni. Among them, the lifetime measurement of the 0_3^+ state is underlined as an accessible and stringent constraint.

ACKNOWLEDGMENTS

This work has been funded by FWO-Vlaanderen (Belgium), by GOA/2010/010 (BOF KU Leuven), by the Interuniversity Attraction Poles Programme initiated by the Belgian Science Policy Office (BriX network P7/12), by the European Commission within the Seventh Framework Programme through I3-ENSAR (Contract No. RII3-CT-2010-262010). This material is based upon work supported by the U.S. Department of Energy, Office of Science, Office of Nuclear Physics under Award No. DE-FG02-94-ER40834, by Spanish MINECO via Project No. FPA2010-17142, by the Slovak grant agency VEGA (Contract No. 2/0121/14), and by the Slovak Research and Development Agency (Contract No. APVV-0177-11).

[1] K. Heyde and J. L. Wood, Rev. Mod. Phys. **83**, 1467 (2011).
[2] A. Andreyev *et al.*, Nature **405**, 430 (2000).
[3] M. Bernas *et al.*, Phys. Lett. B **113**, 279 (1982).
[4] F. Recchia *et al.*, Phys. Rev. C **88**, 041302(R) (2013).
[5] S. Suchyta *et al.*, Phys. Rev. C **89**, 021301(R) (2014).
[6] Y. Tsunoda, T. Otsuka, N. Shimizu, M. Honma, and Y. Utsuno, Phys. Rev. C **89**, 031301(R) (2014).
[7] Y. Tsunoda, T. Otsuka, N. Shimizu, M. Honma, and Y. Utsuno, J. Phys. Conf. Ser. **445**, 012028 (2013).
[8] S. M. Lenzi, F. Nowacki, A. Poves, and K. Sieja, Phys. Rev. C **82**, 054301 (2010).
[9] K. Kaneko, M. Hasegawa, T. Mizusaki, and Y. Sun, Phys. Rev. C **74**, 024321 (2006).
[10] J. Elseviers *et al.* (unpublished).
[11] W. F. Mueller *et al.*, Phys. Rev. C **61**, 054308 (2000).
[12] C. J. Chiara *et al.*, Phys. Rev. C **86**, 041304(R) (2012).
[13] P. Van Duppen, E. Coenen, K. Deneffe, M. Huyse, K. Heyde, and P. Van Isacker, Phys. Rev. Lett. **52**, 1974 (1984).
[14] D. Pauwels *et al.*, Phys. Rev. C **78**, 041307(R) (2008).
[15] B. Zeidman and J. A. Nolen, Jr., Phys. Rev. C **18**, 2122 (1978).
[16] I. Stefanescu *et al.*, Phys. Rev. Lett. **100**, 112502 (2008).
[17] D. Pauwels, J. L. Wood, K. Heyde, M. Huyse, R. Julin, and P. Van Duppen, Phys. Rev. C **82**, 027304 (2010).
[18] A. Dijon *et al.*, Phys. Rev. C **85**, 031301(R) (2012).
[19] R. Broda *et al.*, Phys. Rev. Lett. **74**, 868 (1995).
[20] O. Sorlin *et al.*, Phys. Rev. Lett. **88**, 092501 (2002).
[21] N. Bree *et al.*, Phys. Rev. C **78**, 047301 (2008).
[22] S. Zhu *et al.*, Phys. Rev. C **85**, 034336 (2012).
[23] R. Broda *et al.*, Phys. Rev. C **86**, 064312 (2012).
[24] M. Hannawald *et al.*, Phys. Rev. Lett. **82**, 1391 (1999).
[25] V. N. Fedosseev *et al.*, Rev. Sci. Instrum. **83**, 02A903 (2012).
[26] N. Warr *et al.*, Eur. Phys. J. A **49**, 40 (2013).
[27] D. Radulov *et al.*, Phys. Rev. C **88**, 014307 (2013).
[28] E. A. Mccutchan, Nucl. Data Sheets **113**, 1735 (2012), data extracted from the ENSDF database.
[29] U. Koster, Eur. Phys. J. A **15**, 255 (2002).
[30] S. N. Liddick *et al.*, Phys. Rev. C **85**, 014328 (2012).
[31] J. C. Hardy, L. C. Carraz, B. Jonson, and P. G. Hansen, Phys. Lett. B **71**, 307 (1977).
[32] M. Wang *et al.*, Chin. Phys. C **36**, 1603 (2012).
[33] V. Rahkonen and J. Kantele, Phys. Fenn. **9**, 103 (1974).
[34] D. Pauwels *et al.*, Phys. Rev. C **86**, 064318 (2012).
[35] D. Pauwels *et al.* (private communication).
[36] B. Singh, D. A. Viggars, and H. W. Taylor, Phys. Rev. C **25**, 2003 (1982).